LAWRENCE
LIVERMORE
NATIONAL
LABORATORY

LLNL-TR-686321

Laser Propagation in Nanostructured Ultra-Low-Density Materials

K. B. Fournier, J. Colvin, A. Yogo, G. E. Kemp, H. Matsukuma, N. Tanaka, Z. Zhang, K. Koga, S. Tosaki, H. Nishimura

March 18, 2016

This work performed under the auspices of the U.S. Department of Energy by Lawrence Livermore National Laboratory under Contract DE-AC52-07NA27344.

Laser Propagation in Nanostructured Ultra-Low-Density Materials

K. B. Fournier[1], J. D. Colvin[1], A. Yogo[2], G. E. Kemp[1], H. Matsukuma[2], N. Tanaka[2], Z. Zhang[2], K. Koga[2], S. Tosaki[2], and H. Nishimura[2]

[1] Lawrence Livermore National Laboratory, Livermore, CA, USA

[2] Institute of Laser Engineering, Osaka University, Osaka, Japan

INTRODUCTION

The nanostructure of very-low-density aerogels (< 10 mg/cm^3) affects the laser heating and propagation of the subsequent heat front. Simulations treat these materials as an atomistic medium without any structure differentiating between near-solid-density material and voids. Thus, simulations fail to predict the effects of the aerogel's physical micro or nanostructure on the laser-matter interaction. We have designed an experiment using the GEKKO XII laser and ILE diagnostics to characterize the ionization-wave propagation and x-ray yield from aerogel and mass-matched gaseous targets as the laser passes through each. By design, the gas and aerogel targets will have identical densities and identical effective ionization states.

We have used the GEKKO XII laser facility to test laser propagation in titanium-loaded foams made by LLNL's aerogel synthesis laboratory. [1] The requirements for the underdense aerogel are a density of 2-10 mg/cm^3 to allow laser propagation over a length of the order of 4 mm in a tube of diameter 2 mm. We will observe the effects of the aerogel medium on the heat front propagation and the resulting multi-keV x-ray yield from the target. As a reference, we measure the same propagation and x-ray production from gaseous targets with the same dimensions as the metal-doped aerogels. An example of data showing the effect of foam density on laser heat-front propagation is shown in Fig. 1, taken from Ref. [2]. As the density increases, the laser propagation slows, although the x-ray signal may increase. The current measurements, made with ILE diagnostics, will be an excellent test of simulation codes that model the ionization wave propagation in the low-density media. The measurements will isolate the physics issues that arise in the nanostructured aerogel material but that do not exist in the gas targets. The data will provide experimental verification of theoretical studies [3].

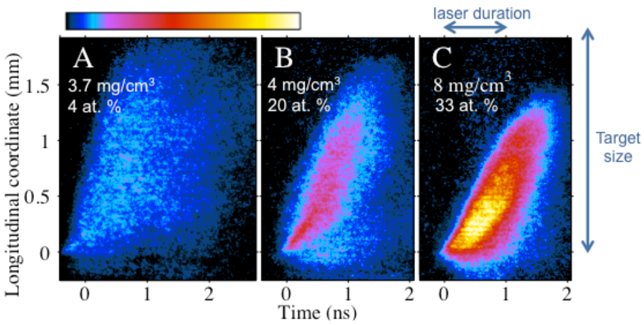

Fig. 1 Streak camera data from three targets of different densities and different nanostructures. The targets extend between 0 and 2 mm. The lasers interact with the targets at 0 mm (taken from Ref. [2]).

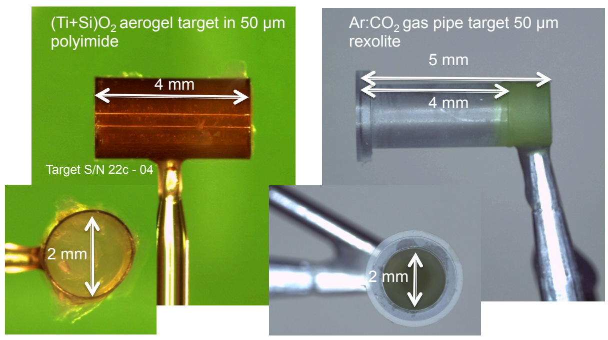

Fig. 2 Side-on and face-on views of the targets used in these laser-propagation studies. (left) Polyimide tube filled with low-density aerogel (right) rexolite gas pipe before being filled. After filling, the window holding the gas in the target bows outwards hundreds of micrometers (not shown in the image above).

EXPERIMENT

Figure 2 shows the two types of targets used in the experiment series. The aerogel material was first cast as pure silica (SiO_2) at a density of 1 mg/cm^3 in polyimide tubes. The aerogel-filled tubes where then coated with titania (TiO_2) using an atomic layer-deposition technique [1,2]. Two batches of targets were produced: 2.6 mg/cm^3 with 18 atom percent Ti and 4.0 mg/cm^3 23 atom percent Ti in a SiO_2 matrix. Our gas targets were produced by General Atomics in La Jolla, CA and had windows and

LLNL-TR-686321

fill tubes mounted by Luxel Corporation. The targets were filled with a mixture of 45% Ar and 55% CO_2 to pressures that ranged between 1.5 atm and 3.0 atm (1140 and 2280 torr). At 1.5 atm, the mass density in the gas is 2.6 mg/cm^3, the same as for the lower-density aerogel targets. In both the case of the aerogel and the gas, for the degree of ionization predicted by simulations, both targets produce plasmas with electron densities approximately 0.1× the critical density for 3ω (351 nm) laser light, and with an average charge on a plasma ion between 10.7 and 11.5 for the aerogel and gas plasmas, respectively. Thus, to a very high degree, the laser sees nearly identical plasmas in either target except for each target's initial nanostructure. Our hypothesis is that any differences in the resulting laser propagation are due to that nanostructure.

These experiments used nine beams of the GEKKO XII laser bundled into a cone and sent to ILE's HYPER target chamber. The bundled beams entered from one side and were incident on one face of the cylindrical targets in a 1.3 ns Gaussian pulse. The lens position of the individual beams was translated up to 5.3 mm to achieve a defocused spot. The resulting laser irradiance on the face of the targets was between 7×10^{14} W/cm^2 and 1.3×10^{15} W/cm^2. The irradiation patter was relatively smooth over a spot ≤ 1 mm in diameter, as calculated geometrically and confirmed by x-ray pinhole images recorded from each target's surface.

An x-ray streak camera was used to determine the plasma heating dynamics. A 15×50 μm^2 slit casts an image of the target from which the central region (along the cylinder axis) was selected on a CsI cathode with a < 50 μm resolution. Streaking this one-dimensional image then provided a temporal resolution < 0.1 ns. Data from streaked records of an aerogel target (top) and a gas-pipe target (bottom) are shown in Fig. 3. Emission starts a few hundred picoseconds after the start of the laser pulse, corresponding to an initial heating and ionization phase. The emission extends spatially nearly the entire length of the 4 mm gas-filled target. It should be noted in the Ar data that once can clearly see the shadow of the washer that holds the window that keeps the gas in the target. The (bright) emission that is to the left of the washer comes from the gas that is in the window when the window is bowed several hundred micrometers beyond the edge of the target. The level of contrast between the emission from this window bubble and the main body of the gas pipe indicates how strongly absorbing the gas-pipe material is of the Ar K-shell x rays.

A qualitative comparison of the propagation results is shown in Fig. 3 for a 2.6 mg/cm^3 Ti-doped aerogel and 45% Ar-55% CO_2 target at a fill pressure of 1.5 atm. Both targets were shot at maximum energy with the GEKKO XII beams defocused by ≈5300 μm. The irrdiance at the face of the targets was $\approx8.5\times10^{14}$ W/cm^2. Our initial estimates of the laser-heating propagation velocity, as given by the position of the x-ray emission on the streak camera's detector, differ by a factor of ten. Generally, this observation holds for all aerogel and gas targets at comparable densities: the propagation of the laser heating in the gas is between 5 and 10× faster than in the aerogels. We note the estimated velocity of laser propagation in the aerogel target, 0.76 mm/ns, is comparable to other measurements we've made at similar densities: 1.4±0.2 mm/ns for 4 mg/cm^3 ALD titania-coated foams [2], ≈ 1±0.3 mm/ns for 2 mg/cm^3 SiO_2 [4], 0.48 mm/ns with a lower laser irradiance for 3 atom percent Ti in 3.2 mg/cm^3 metal-doped SiO_2 [5].

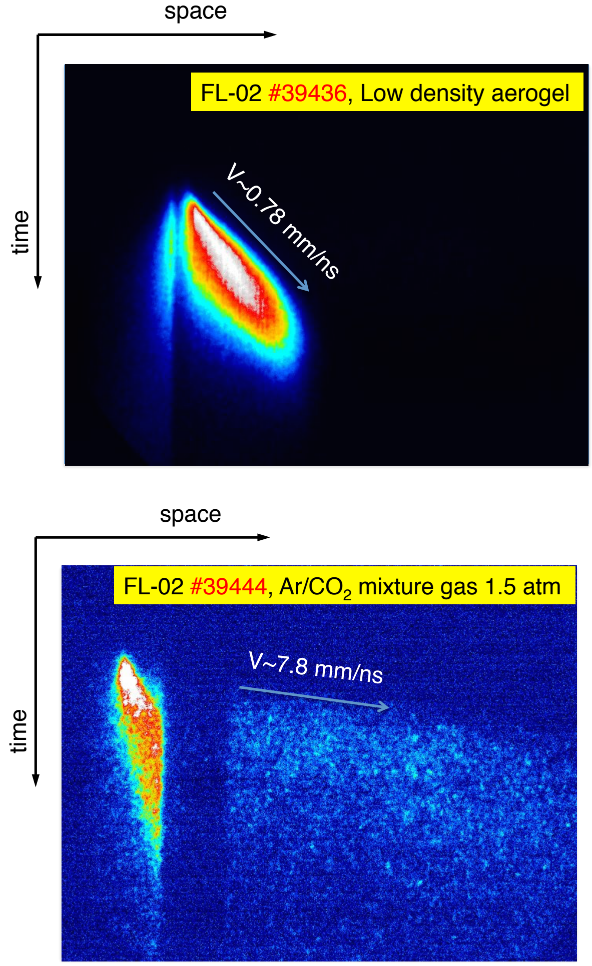

Fig. 3 Streak camera data from (top) a Ti-coated SiO2 aerogel target (2.6 mg/cm^3) and (bottom) a 1.5 atm 45:55 Ar:CO_2 gas target. The two targets had equal density, and are predicted to have equal plasma electron density.

An additional assessment of the laser heating of the plasma can be obtained from x-ray spectra measured on each shot. A crystal spectrometer was fielded that provided a view of each target perpendicular to the target's cylindrical axis. Thus, the spectrometer looked through the target wall (polyimide for aerogels, rexolite for the gas targets) to measure K-shell x-rays from the heated plasma. Figure 4 shows spectra from an aerogel and a gas target. The plasma temperature can be estimated by the ratio of H-like x rays (the Ly-α feature) to the He-like (He-α) x rays. The spectra shown in Fig. 4 have not had the effect of the target-wall-material opacity taken out of the data, thus the absolute levels of the line strengths shown are not meaningful. The Ar He-α complex is much better resolved than the equivalent complex in the Ti spectrum. The strength of the Ti Lyα line above background is significantly better than in the case of Ar Ly-α. However, until target opacity effects are removed from the data, no conclusions about plasma electron temperatures can be drawn at this time. Collisional-radiative modeling will be performed to understand the temperature dependence in the measured spectra.

SUMMARY

We have measured laser propagation in ultra-low-density materials heated by the GEKKO XII laser. The targets were shot in the HYPER chamber with nine of the GEKKO beams bundled and incident from one side of the target. A streaked record was made of the x-ray emission from the target as the laser propagated down the target's cylindrical axis. The targets were designed to have the same mass density, effective ionization state and electron density for both the aerogel and gas specimens. Thus, differences in the propagation of the laser heating are most likely due to the difference in target nanostructure for the aerogel versus the atomostically mixed materials in the gas targets. We observe 5 to 10× faster propagation in the gas targets than in the corresponding aerogels. This assessment is, at the moment, only qualitative and further quantitative analysis is in progress. The challenge is now for radiation-hydrodynamics codes to develop a numerical treatment for the aerogel nanostructure that allows the codes to reproduce this difference between the gas and aerogel propagation differences.

ACKNOWLEGEMENT(S)

This work was performed under the auspices of the U.S. Department of Energy by Lawrence Livermore National Laboratory under Contract No. DE-AC52-07NA27344.

REFERENCE(S)

[1] M. M. Biener *et al.*, Atomic Layer Deposition-Derived Ultra-Low-Density Composite Bulk Materials with Deterministic Density and Composition, *Appl. Mater. Interfaces* **5**, 13129-13134 (2013).
[2] F. Pérez *et al.*, Bright x-ray sources from laser irradiation of foams with high concentration of Ti, *Physics of Plasmas* **21**, 023102 (2014).
[3] S. Yu. Gus'kov *et al.*, Laser-supported ionization wave in under-dense gases and foams, *Phys. Plasmas* **18**, 103114 (2011).
[4] M. Primout *et al.*, A new hybrid target concept for multi-keV X-ray sources, *High Energy Density Physics* **9**, 750-760 (2013).
[5] M. Tanabe *et al.*, Characterization of heat-wave propagation through laser-driven Ti-doped underdense plasma, *High Energy Density Physics* **6**, 89-94 (2010).

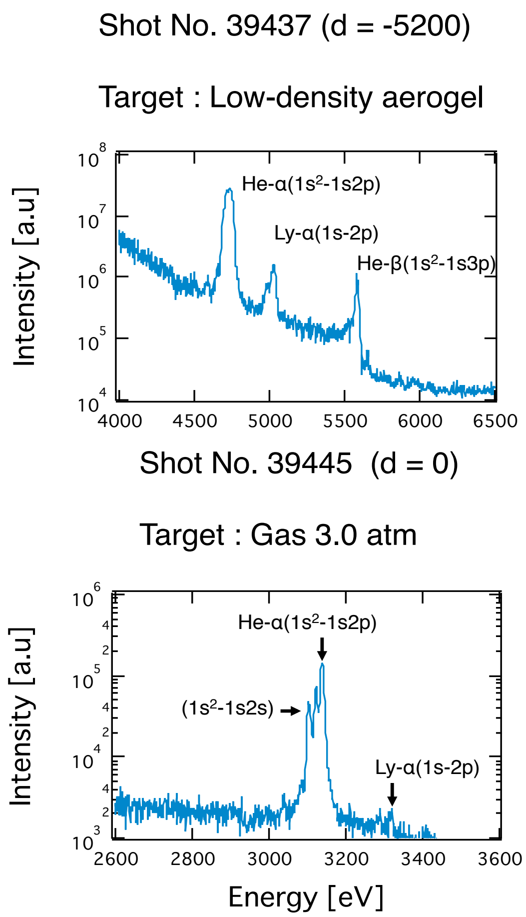

Fig. 4 X-ray spectra from (top) a Ti-coated aerogel target and (bottom) a Ar:CO_2 gas target.